Passage of uncharged dextrans from blood to lung lymph in awake sheep

PAUL N. LANKEN, JOHN H. HANSEN-FLASCHEN, PHYLLIS M. SAMPSON, GIUSEPPE G. PIETRA, FREDERICK R. HASELTON, AND ALFRED P. FISHMAN
Cardiovascular-Pulmonary Division, Department of Medicine and Division of Anatomic Pathology, Department of Pathology and Laboratory Medicine, University of Pennsylvania School of Medicine, Philadelphia, Pennsylvania 19104

LANKEN, PAUL N., JOHN H. HANSEN-FLASCHEN, PHYLLIS M. SAMPSON, GIUSEPPE G. PIETRA, FREDERICK R. HASELTON, AND ALFRED P. FISHMAN. *Passage of uncharged dextrans from blood to lung lymph in awake sheep.* J. Appl. Physiol. 59(2): 580–591, 1985.—To examine how molecular size alone influences the passage of macromolecules from the pulmonary microcirculation into lymph collected from the caudal mediastinal lymph node of the sheep, we infused polydisperse uncharged [^{3}H]dextrans intravenously at a constant rate over a period of 7.5 h in nine awake sheep with lung lymph fistulas. Lymph and plasma were collected during *hours 5.5–7.5* of the infusions, and the [^{3}H]dextrans were separated by molecular sieve chromatography into fractions that ranged from 1.6 to 8.4 nm in effective molecular (Stokes-Einstein) radius. Lymph-to-plasma (L/P) ratios for [^{3}H]dextrans were near 1.0 at 1.6-nm radius, decreased with increasing molecular size, and approached zero at radii above 5.0 nm. We confirmed that these L/P ratios represented steady-state values by extending the duration of the infusion to ~30 h in two of the nine sheep and finding that the L/P ratios remained unchanged. These results were consistent with molecular sieving through a homoporous membrane with cylindrical pores of 5.0-nm radius. We also found that the L/P ratio for albumin [0.76 ± 0.13 (SE)] in five of the same sheep was much higher than that for the [^{3}H]dextran fraction of the same effective molecular radius [0.11 ± 0.02 (SE)]. These results suggest that the movement of macromolecules from the pulmonary microcirculation into pulmonary lymph collected from the caudal mediastinal node of the sheep is influenced by both molecular size and molecular charge and that, compared with uncharged dextrans, the steady-state passage of anionic endogenous proteins from plasma to lymph is enhanced.

capillary permeability; endothelium; macromolecules; pulmonary edema; permselectivity; mathematical model; pulmonary microcirculation

COMPARISONS of lymph-to-plasma concentration ratios (L/P ratios) for endogenous protein fractions of graded molecular size have suggested that transendothelial passage of macromolecules involves sieving according to molecular size. This conclusion is based on observations in awake sheep with chronic lung lymph fistulas (4) and on anesthetized open-chest dogs in which lymph was collected from prenodal lobar lymphatics (30). In these studies, although the L/P ratios for most of the endogenous plasma protein fractions decreased as their effective molecular (Stokes-Einstein) radii increased, the possibility arises that the electrical charge of the test macromolecules, as well as their effective molecular size, could have influenced their steady-state passage from plasma to lymph. This prospect seems plausible on two grounds: *1*) at physiological pH virtually all plasma proteins have a net negative charge [e.g., the isoelectric point of albumin is 4.7 (33)]; and *2*) electrical charge has been shown to influence the transcapillary passage of macromolecules in renal glomerular capillaries (5). Previous observations from this laboratory (22, 32) and elsewhere (15) are in accord with this possibility.

The present study, based largely on the use of uncharged macromolecules infused into intact unanesthetized sheep with fistulas designed to collect pulmonary lymph, was undertaken to examine how macromolecular size, per se, influences the passage of the macromolecules across the pulmonary microcirculation and to compare the steady-state L/P ratios of these uncharged solutes with those of charged macromolecules of the same effective molecular size.

Our results indicate that the uncharged macromolecules pass from endothelium via interstitium to the lymph-collecting site as though passing through a homoporous membrane permeated by water-filled cylindrical pores, ~5.0 nm in radius. Comparison of L/P ratios for uncharged dextrans with those for anionic plasma proteins of the same effective molecular radii also suggest that the steady-state passage of anionic macromolecules from the pulmonary microcirculation to lymph is greatly enhanced compared with that of uncharged macromolecules.

MATERIALS AND METHODS

Animal Preparation: Awake Sheep with Chronic Lung Lymph Fistulas

Experiments were done on male sheep 32–52 kg in wt and 6–12 mo of age. To minimize the risk of contamination of lung lymph from extrapulmonary sources (34), the original method of Staub et al. (38) was modified,

using four separate thoracotomies in each sheep to accomplish the following. *1*) The anastamoses were interrupted between systemic lymphatics and the caudal mediastinal lymph node; this was accomplished by resecting the caudal mediastinal lymph node in the standard way (38) followed by ligation or cauterization of right and left diaphragmatic lymphatics visualized by injecting Evans blue dye (25 mg) in 10–15 ml of 0.9% saline at multiple sites in the right and left hemidiaphragms. *2*) Hemodynamic variables were monitored; for this purpose we placed silicone hemodynamic catheters [0.062 in. (ID), 0.125 in. (OD), Dow Corning] in the main pulmonary artery and left atrium, marking the horizontal level of the dorsal aspect of the left atrium on the external surface of the thorax for reference; we placed additional catheters in the superior vena cava via the right external jugular vein and in the aorta via the right common carotid artery. *3*) The efferent lymphatic duct from the caudal mediastinal lymph node was cannulated in the standard manner (38).

We administered antibiotics prophylactically both during the operation and for 48 h postoperatively; gentamycin 2.5 $mg \cdot kg^{-1} \cdot day^{-1}$ in two doses intramuscularly and chloramphenicol 2 g/day in two doses intravenously. We flushed the hemodynamic catheters twice a day with sterile 0.9% saline containing heparin (100–200 U/ml).

We waited 7–10 days after the four thoracotomies had been completed until pulmonary lymph flow became stable and blood free by visual inspection of the pellet after centrifugation. Our experiments were carried out in nine sheep prepared in this manner. On the day of the experiment base-line values (means ± SD) in these nine sheep were as follows: body temperature, 39.4 ± 0.3°C; arterial pH, 7.54 ± 0.031; arterial P_{O_2}, 88.0 ± 7.4 Torr; arterial P_{CO_2}, 32.0 ± 3.7 Torr.

Preparation of [^{3}H]dextran

Dextran T500 [Lot 11648, with molecular weights of 461,000 (wt avg) and 180,000 (no. avg), Pharmacia Fine Chemicals, Piscataway, NJ] was covalently labeled with tritium, using a modification of the oxidation-reduction procedure of Chang et al. (6). The following steps were involved. For each tritiation 200 mg of dextran T500 were dissolved in 2 ml of water prior to addition of 1 ml of sodium metaperiodate at a concentration of 105 mg/ml. Oxidation was conducted for 3.5 h in the dark at room temperature, after which 0.5 ml of 0.5 M barium acetate was introduced and the reaction mixture was cooled to 4°C for 10 min to precipitate the barium salts. After the mixture was centrifuged for 10 min, 3 vol of absolute ethanol were mixed with the supernatant; the mixture was kept at 4°C overnight. The resulting precipitate was collected by centrifugation at 5°C and redissolved in 5.0 ml of water containing two drops of concentrated ammonium hydroxide; it was then transferred to a 100-ml round-bottom 24/40 flask. Within an airhood, two or three vials of tritiated sodium borohydride (5 mCi each, 348.7 mCi/mmol, New England Nuclear, Boston, MA) were added to the flask. After the mixture reacted for 10 min at room temperature 50 mg of cold sodium borohydride (Aldrich Chemical Co., Milwaukee, WI) were added. After 1 h 50 mg more of cold sodium borohydride were added, and after 2 additional h, to decompose the unreacted borohydride, glacial acetic acid (~4–5 ml) was pipetted in slowly until no more bubbles formed. After being mixed with 10 ml of absolute methanol the solution was evaporated to 1–2 ml by use of a rotary evaporator. To this residue were added sequentially 1.0 ml of water, glacial acetic acid to a final pH of 4, and 10 ml of absolute methanol. The sample was then reevaporated three times in the same manner as above. The final dried sample was dissolved in 10 ml water, dialyzed overnight at 4°C against 1 liter of water containing chloroform, and lyophilized for storage at room temperature in a desiccator over calcium chloride. The final yield varied from ~60 to 120 mg. That the tritium label on the dextran was stable chemically was demonstrated by the final specimen having constant specific activity after repeated lyophilizations.

For this procedure we used only analytical reagent-grade chemicals, sterile pyrogen-free water, and sterile plasticware or acid-washed glassware in order to prevent contamination of the [^{3}H]dextrans with endotoxin. We excluded the presence of endotoxin in samples of all [^{3}H]-dextran preparations by use of a *Limulus* assay (Amebocyte Lysate Kit, Difco Laboratories, Detroit, MI).

Characterization of [^{3}H]dextrans

Lack of electrical charge. To confirm that the [^{3}H]-dextrans that we prepared were uncharged we performed electrophoreses using cellulose acetate at two different pH values. The first electrophoresis was done at pH 8.6 in 0.075 M barbital buffer and used plasma proteins and glycosaminoglycans as anionic markers. After electrophoresis we stained the cellulose acetate strip with alcian blue to identify glycosaminoglycans or with Ponceau S to identify proteins. We cut each electrophoretogram into portions corresponding to the origin, the plasma protein area, and the glycosaminoglycan area, and after extraction in 0.1 M sodium hydroxide overnight we analyzed each portion for radioactivity using standard techniques as described below. We found that 100% of the radioactivity of [^{3}H]dextran sample remained at the origin, indicating the lack of a net electrical charge at pH 8.6. To rule out the possibility that the [^{3}H]dextrans were at their isoelectric point and thus had no net electrical charge at pH 8.6, we repeated the electrophoresis at a different pH. The second electrophoresis was carried out at pH 3.5 in 1 M acetate buffer containing pyridine (6 ml/l of buffer). We used glycosaminoglycans as anionic markers and cytochrome *c* as a cationic marker. We again found that virtually all of [^{3}H]dextran radioactivity remained at the origin, confirming the lack of any electrical charge.

Distribution of molecular sizes. The distribution of effective molecular sizes of each [^{3}H]dextran preparation was determined by molecular sieve chromatography. Approximately 0.5 μCi of [^{3}H]dextran in 2.0 ml of buffer was applied to columns prepared and calibrated as described below. From each fraction a 1.0-ml aliquot was

added to 5.0 ml of liquid scintillation fluid (Aqualyte Plus, Baker Chemical, Phillipsberg, NJ). Radioactivity in counts per minute (cpm) was measured in a liquid scintillation counter as the mean of four 1-min counts minus the mean background count. The mean background count was determined in an identical manner, using 1.0-ml aliquots from one or more fractions that had elution volumes less than the void volume of the column. The peaks of the distribution of the [^{3}H]dextran preparations occurred in fractions of 3.5–4.5 nm in effective molecular radii. These were smaller than the peak of distribution of the Dextran T500 used as substrate for the tritiation and may be attributable to oxidative cleavage of glycosidic bounds (6) and/or conformational changes in the dextran polymer due to opening of its hexose rings.

To test the inherent variability of the molecular sieve chromatographic column we applied replicate samples of the same [^{3}H]dextran preparation to the same column over a 1-mo period and determined the reproducibility of the elution patterns for the [^{3}H]dextrans as described above. We found that the elution patterns were virtually identical except for shifts of the pattern up to one fraction; i.e. the peaks in the distribution of molecular sizes of replicate samples occurred in the same fraction or in the next preceding or following fraction. We considered this range of shifts to represent the inherent variability of our columns. The mean overall coefficient of variation for replicate column fractionations of [^{3}H]dextran was 7.3%. In addition the column was tested for another aspect of reproducibility by rechromatography of individual fractions of [^{3}H]dextrans. For this purpose aliquots of eight fractions of [^{3}H]dextrans selected over a range of molecular sizes from ~1.6 to 8.4 nm in radius were reapplied to the same column and radioactivity in the eluted fractions was determined as above. Rechromatographed aliquots from all eight fractions retained peaks of radioactivity in their original fractions.

We also determined that the tritium labeling of the dextran fractions was uniform by comparing the relative distribution of radioactivity among fractions with the relative distribution of carbohydrate content among the same fractions by means of the anthrone reaction (11) (using glucose as standard followed by measuring absorbance at 620 nm). We found that the two patterns of distribution were virtually identical.

In addition we evaluated whether fractions of the [^{3}H]-dextrans might bind either to endogenous macromolecules in sheep plasma or lung lymph or to the molecular sieve chromatographic column itself. The former prospect was tested by comparing the distribution of molecular sizes resulting from fractionation by column of replicate samples of the same lot of [^{3}H]dextran dissolved separately in 2 ml of buffer, in heparinized sheep plasma or in lung lymph. The lack of tracer binding to endogenous macromolecules was confirmed by finding no differences in results among these three distributions. The possibility of [^{3}H]dextran binding to the column was evaluated by applying separately the following quantities of the same [^{3}H]dextran preparation in 2 ml of buffer to the same column: 0.06, 0.24, 1.2, and 12 μCi. The smallest quantity corresponded to the order of magnitude of our experiment lymph and plasma specimens. Lack of interaction between even the small quantities of [^{3}H]dextran used and the column was indicated by the following results: total recoveries were virtually 100% (range = 97–113%); all four quantities of the [^{3}H]dextran eluted with the peak of its distribution in the same fraction; and all four quantities had virtually the same proportion of total [^{3}H]dextran eluting in fractions >4.8 nm in radius.

Preparation and Calibration of Molecular Sieve Chromatographic Columns

After equilibrating columns of Sephacryl S-300 (Pharmacia Fine Chemical) (~50 cm long, 1.6 cm in diam) in at least five column volumes of 0.006 M phosphate buffer, pH 7.5, containing 0.15 M sodium chloride (to approximate physiological pH and ionic strength) and 0.02% sodium azide, we calibrated columns using Blue dextran (Pharmacia Fine Chemicals) and a series of globular proteins, (Table 1); all of these reagents except cytochrome *c* (Calbiochem-Behring, La Jolla, CA) were obtained from Pharmacia Fine Chemicals. After samples were applied separately in 2 ml of buffer the columns were eluted with buffer at a flow of 0.5–0.8 ml/min at a constant hydrostatic pressure (123 cmH_2O); the eluate was collected in 1.6-ml fractions. For all calibrating markers we measured their absorbance at 280 nm in aliquots of column fractions and determined their elution volumes by identifying the peak of their absorbances. We determined the fraction of the total volume of the column available for equilibration (k_{av}) for each calibrating protein (24) on the basis of the determined elution volumes, by assuming the elution volume of Blue dextran as the void volume of the column, and by calculating the total volume of the column from its calculated dimensions. We also calculated the effective molecular radius of each calibrating protein by the Stokes-Einstein equation, using published data for the free diffusion coefficient of each protein (Table 1).

By applying the method of least squares to the data

TABLE 1. *Free diffusion coefficients and effective molecular radii of calibrating proteins*

Calibrating Protein	$D^0_{20,w}$, $cm^2 \cdot s^{-1} \times 10^7$	Ref. No.	Effective Molecular Radius,* nm
Cytochrome *c*	13.0	1	1.65
Ribonuclease A	10.68	7	2.01
Chymotrypsinogen A	9.5	37	2.26
Ovalbumin	7.8	21	2.75
Bovine albumin	6.0	39	3.57
Aldolase	4.6	43	4.66
Catalase	4.1	40	5.23
Ferritin	NA		6.10†
Thyroglobulin	2.5	12	8.57

NA, not applicable; $D^0_{20,w}$, free-diffusion coefficient of protein in water at 20°C. *Effective molecular radius was calculated by use of Stokes-Einstein equation, $D^0_{20,w} = kT/6\pi\eta \cdot a_s$, where k is Boltzmann constant; T is absolute temperature; η is viscosity of water; and a_s is solute's effective molecular radius, i.e., Stokes-Einstein hydrodynamic radius. † Value from X-ray diffraction analysis (46).

relating k_{av} of each protein and the logarithm of its effective molecular radius (24), we derived a linear regression equation to calibrate each column. From this equation we calculated effective molecular radii for the midpoints of elution fractions over the size range of our calibrating proteins. Eleven separate calibrations were done on six different chromatographic columns during the course of these experiments. The mean correlation coefficient for the regression equation used in calibration was −0.9931 (range −0.9899 to −0.9986).

Finally, we confirmed that our calibration, based on the effective molecular radii of the calibrating globular proteins, was also accurate for use with dextrans by appling a sample of Dextran T40 [Lot 7974 and mol wt of 41,500 (wt avg) and 26,800 (no. avg), Pharmacia Fine Chemicals] whose peak fraction by weight had a known effective molecular radius, 4.45 nm (courtesy of Charles Mason of Pharmacia Fine Chemicals). On our column the peak of this dextran as determined by means of the anthrone reaction (11), eluted in a fraction whose mean effective molecular radius as determined by our calibration was 4.32 nm, a difference that represented a shift of less than one column fraction and thus fell within the inherent variability of the column as described above.

Experimental Procedure

Control period. After sheep had been prepared as described above control observations were obtained over a period of 1.5–3.0 h immediately prior to the test period. During this interval the sheep were awake and standing within metabolic cages that allowed free access to food and water. Hemodynamic measurements were made of systemic arterial, pulmonary arterial, and left atrial mean pressures except for omission of pulmonary arterial pressure in one sheep due to an occluded catheter. Pressures were obtained using Statham P23Db pressure transducers, an electronic amplifier, and a recorder and printer (Electronics for Medicine). Arterial blood samples were taken for pH, P_{O_2} and P_{CO_2} measured at 37°C by use of a Corning 175 blood gas analyzer. In the two sheep receiving infusions of ~30 h in duration we also determined the mean cardiac output as an average of three trials of the thermodilution method. For this purpose a flotation catheter (model 93A-131-7F, American Edwards Laboratories, Irvine, CA) was introduced in the pulmonary artery, and cardiac output was determined using a computer (model 9520A, American Edwards Laboratories) following injection of cold saline into the right atrium. Lymph was collected continuously at 30- to 60-min intervals into 15-ml sterile graduated plastic centrifuge tubes for measurement of volume (Corning Glass Works, Corning, NY); the tubes contained 500–1,000 U of heparin sodium. In some of the animals aliquots of pooled lymph and arterial plasma taken at the beginning and end or at the midpoint of a lymph collection period were used to determine L/P ratios for total protein and albumin concentrations. For the determination of total protein concentration the aliquots of lymph and plasma were stored at 5°C and assayed within 3 days after collection. Total protein concentration was measured in duplicate using the biuret method (9) and bovine albumin (Stanbio Laboratory, San Antonio, TX) as a standard. Values for duplicate specimens varied by a mean difference of 4.8%. Aliquots for albumin determinations had 20 μl of a 5% solution of sodium azide added per 6 ml of sample before storage at 5°C. Albumin concentrations were determined in duplicate specimens by radial immunodiffusion (25), using ovine albumin (Sigma Chemical, St. Louis, MO) as a standard. Values for duplicate specimens varied by a mean difference of 4.0%.

Test period. During the test period the sheep remained in a metabolic cage, free to eat and drink. We started the infusion of the [^{3}H]dextran immediately at the end of the control period after the lymph flow and hemodynamic measurements had become stable. The [^{3}H]dextrans (sp act 40–113 μCi/mg) were dissolved in sterile pyrogen-free 0.9% saline and infused by a constant-flow infusion pump (model 2205, Harvard Apparatus, South Natick, MA), using a sterile 50-ml plastic syringe; the infusate was delivered into the superior vena caval catheter via a sterile plastic extension tubing and a 0.22-μm sterile filter (Gelman Instrument, Ann Arbor, MI).

In each of the nine sheep an initial loading dose of the [^{3}H]dextran was followed by a continuous base-line infusion rate of ~0.15 $\mu Ci \cdot kg^{-1} \cdot min^{-1}$. The loading dose was given by one of two methods. The first four sheep received a bolus injection of ~10 μCi/kg. This injection produced initial levels of radioactivity in plasma far in excess of subsequent steady levels achieved by constant infusion. To avoid this overshoot in plasma radioactivity, loading in the other five was accomplished in two steps during the first 0.5 h: by infusion of [^{3}H]dextran at four times the base-line rate during the first 15 min, two times the base-line rate during the second 15 min, and thereafter at the base-line rate. Since both types of loading resulted in no statistically significant differences in mean L/P ratios between groups for any fraction from samples collected over our standard collection period of 5.5–7.5 h of infusion, we combined the groups for analysis. The base-line infusion rate of 0.15 $\mu Ci \cdot kg^{-1} \cdot min^{-1}$ was chosen because in preliminary experiments that rate provided plasma levels of [^{3}H]dextran in all fractions which remained virtually constant over *hours 3.5–7.5* of the infusion and were sufficiently high to ensure accurate counting. The final plasma activity was of the order of 50,000 cpm/ml or ~0.06 μCi/ml.

During the first 1.5 h, the volume of lymph flow and hemodynamic measurements were made at 15- to 30-min intervals and repeated subsequently at 1- to 2-h intervals for 7.5 h. This pattern of sampling was identical to that of the control period. Similarly lymph and blood were sampled at the same regular intervals as during the control periods for the determination of the concentrations of total protein and albumin in lymph and plasma.

The [^{3}H]dextran infusions were continued for at least 7.5 h in all nine sheep. In four of the nine the infusions were continued at the same rate and under the same experimental conditions beyond 7.5 h to test whether full equilibration of the tracer between plasma and lymph had occurred by 7.5 h; in these four sheep the infusions were continued for 13, 15, 29.5, and 30.5 h, respectively.

In the two sheep receiving the infusions of the longest duration during the standard 5.5- to 7.5-h collection period and during the final collection period, we repeated measurements of body temperature, arterial pH, P_{O_2}, and P_{CO_2}, and cardiac outputs in the same manner as in the control period.

For all nine sheep we collected at 1- to 2-h intervals all lymph produced during the 4 h between 3.5 and 7.5 h of infusion. We also collected arterial blood samples at the beginning and end (for averaging) or at the midpoint of each lymph sample collection period in order to determine the L/P ratios for the fractions of [^{3}H]dextrans as described below. We sampled over this 4-h period in order to test whether the L/P ratios for all fractions were unchanging over this 4-h period, i.e., were consistent with full equilibrium of the dextran fractions between plasma and lymph. The specimens of lymph and blood were collected, processed, and stored as described above for the control period.

Lymph-to-Plasma Ratios and Calculations

Two milliliters of a lymph and a corresponding plasma sample were alternatively applied to a calibrated chromatographic column, and the eluate was collected in 24–26 1.6-ml fractions over a range of effective molecular radii of ~1.6–8.4 nm. From each fraction a 1.0-ml aliquot was added to 5.0 ml of scintillation fluid, and its radioactivity was determined using a liquid scintillation counter by the same method as described above. Duplicate lymph and plasma samples were applied to the column in reverse of the order used for the first pair of samples. The degree of quenching was found to be the same for fractions of lymph or plasma. The corresponding mean background counts per minute, determined as described above, was subtracted from the counts per minute of each fraction prior to L/P ratio calculations. The concentration of [^{3}H]dextran in each plasma fraction was sufficiently high to ensure accurate counting; the lowest radioactivity in any fraction of the plasma samples averaged 16 times (range 5.3–47.3 times) greater than the background counts per minute. A mean L/P ratio for each [^{3}H]dextran fraction of each infusion was calculated by dividing the mean counts per minute for the lymph specimens obtained during a specific time period of the infusion by the mean counts per minute of the corresponding plasma samples. Because samples from the nine infusions were fractionated on different columns, L/P ratios were obtained at the same exact radii by linear interpolation.

To test whether the mean L/P ratios of the fractions of [^{3}H]dextran from samples collected during our standard collection period (*hours 5.5–7.5* of infusion) varied with time, two comparisons were made before and after this period. First, mean L/P ratios were calculated for each radius, using the samples collected during *hours 3.5–5.5* of eight of the nine infusions (in one sheep these specimens were lost) and compared with those from samples collected during *hours 5.5–7.5* of the same infusions. Second, for the four extended infusions L/P ratios were calculated at each radius for their final lymph collection period (11.5–13.0, 14.5–15.0, and 27.5–29.0 h, and 29.5–30.5 h, respectively); these latter L/P ratios were compared with the mean L/P ratios from the 5.5- to 7.5-h period of infusion for the same sheep that had received the extended infusions.

Mathematical Modeling

We determined how closely the data relating steady-state ratios for [^{3}H]dextrans and their effective molecular radii could be described by a mathematical model in which molecular sieving was postulated to occur through a semipermeable membrane containing cylindrical pores of a single radius, i.e., a single pore model. Details of the assumptions, equations, and methods used for this determination are given in the APPENDIX.

Statistical Analysis

Data are presented as means ± SE unless otherwise indicated. Correlation coefficients for linear regression equations used to calibrate the chromatographic columns were derived by use of the statistical programs of a desk calculator. To compare means of lymph, plasma, and hemodynamic parameters between control and test periods, the Student's t test for paired observations was used. The latter was also employed to compare L/P ratios for [^{3}H]dextran fractions taken over 3.5 to 5.5 h of infusion with those taken during 5.5–7.5 h of infusion.

We compared mean L/P ratios for [^{3}H]dextran fractions among those receiving the two different types of loading doses by the Student's t test for unpaired observations. The latter was also employed to compare L/P ratios of albumin or other endogenous protein fractions with those of [^{3}H]dextran fractions at the same or slightly greater radius.

For all comparisons we interpreted $P < 0.05$ as significant.

RESULTS

Infusion of Uncharged [^{3}H]dextrans

Infusion of uncharged [^{3}H]dextran for 7.5 h had no effect on lymph, plasma, or hemodynamic parameters for the nine sheep, as shown in Table 2. None of the differences in means between control and test period (*hours 5.5–7.5* of the infusion) were statistically significant. In addition, in the two sheep that received the extended infusions to 29.5 and 30.5 h, we found virtually no change in these parameters or in arterial P_{O_2}, P_{CO_2}, and pH, or body temperature and cardiac output when the control period was compared with the 5.5- to 7.5-h test period and final 1- to 1.5-h period of each infusion.

Representative Infusion and Validation of Steady State

Figure 1 shows L/P ratios of [^{3}H]dextrans according to effective molecular radius for 5.5–7.5 h of infusion for a representative single sheep. Also shown for comparison are the L/P ratios obtained from 17.5 to 18.5 and 29.5 to 30.5 h of the same constant infusion of [^{3}H]dextran in

TABLE 2. *Lymph, plasma, and hemodynamic parameters in control and test periods*

	Control Period	Test Period*
Lymph flow, ml·h^{-1}	7.1±1.5 (9)	7.4±1.5 (9)
Lymph total protein, g·dl^{-1}	3.79±0.26 (6)	3.64±0.18 (6)
Plasma total protein, g·dl^{-1}	5.91±0.40 (6)	6.00±0.25 (6)
L/P ratio, total protein concentration	0.63±0.02 (6)	0.60±0.03 (6)
Lymph albumin, g·dl^{-1}	1.75±0.13 (5)	1.71±0.15 (5)
Plasma albumin, g·dl^{-1}	2.34±0.15 (5)	2.21±0.18 (5)
L/P ratio, albumin concentration	0.75±0.04 (5)	0.76±0.01 (5)
Heart rate, min^{-1}	110±6 (9)	112±6 (9)
Systemic arterial pressure (mean), Torr	93.3±4.4 (9)	94.5±3.1 (9)
Pulmonary arterial pressure (mean), Torr	16.3±0.9 (8)	16.8±0.9 (8)
Left atrial pressure (mean), Torr	3.8±0.5 (9)	4.0±0.6 (9)

Values are means ± SE for no. of sheep given in parentheses. L/P, lymph-to-plasma ratio. * *Hours 5.5–7.5* of [^{3}H]dextran infusions.

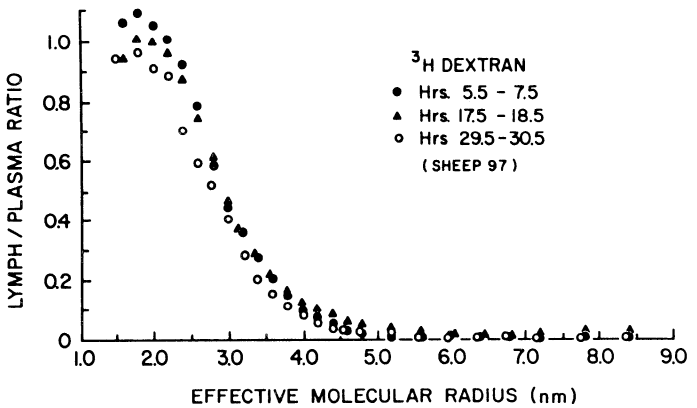

FIG. 1. Lymph-to-plasma (L/P) ratios of [^{3}H]dextran fractions according to effective molecular radii from an infusion in single representative sheep (*97*). L/P ratios from samples obtained during 5.5–7.5 h of infusion are compared with values obtained during 17.5–18.5 h and 29.5–30.5 h and indicate that within limits of variability of technique no change in L/P ratios occurred over time. Pattern of L/P ratios vs. effective molecular size is consistent with molecular sieving of tracer from plasma to lymph.

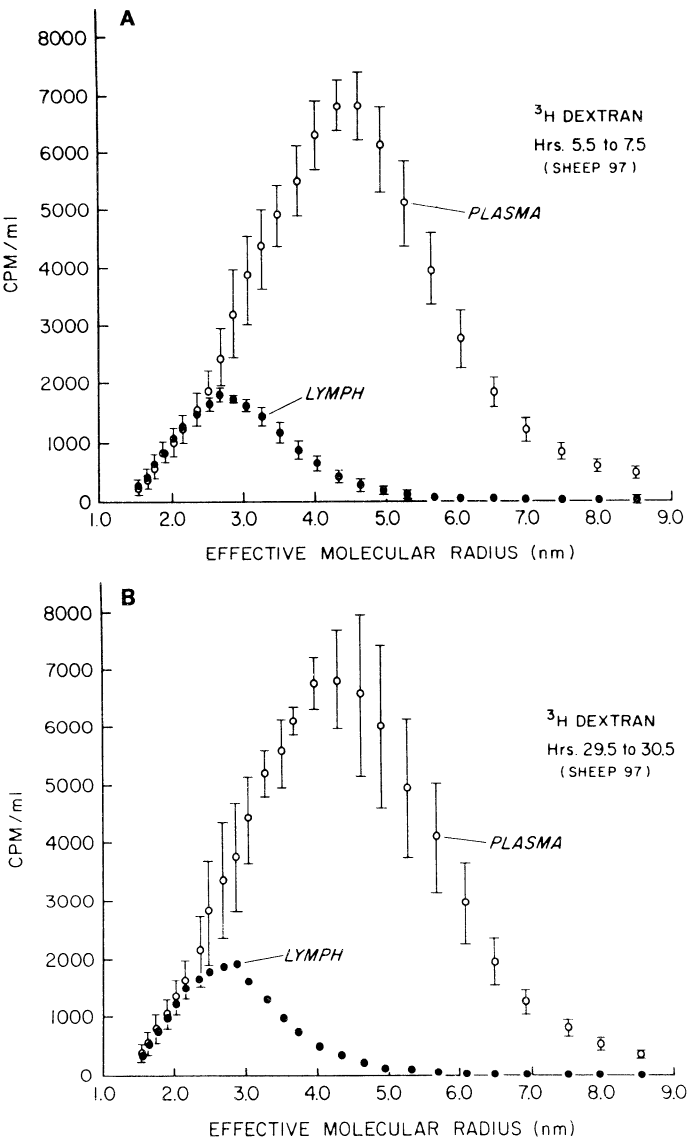

FIG. 2. *A*: differences between concentrations of [^{3}H]dextran fractions in plasma and lymph specimens obtained during *hours 5.5–7.5* of [^{3}H]dextran infusion in single representative sheep from which lymph-to-plasma (L/P) ratios shown in Fig. 1 were derived. Each *point* represents mean cpm/ml (±SD) per fraction from 2 hourly lymph samples and corresponding plasma samples (taken at midpoint of each lymph collection period) both fractionated in duplicate. Polydisperse nature of tracer can be seen by its distribution in plasma; lymph data are consistent with molecular sieving of tracer from plasma to lymph. In addition, it can be seen that very low lymph-to-plasma (L/P) ratios calculated for fractions >5.0 nm in radius (Fig. 1) result from low concentrations of tracer in lymph rather than from very high plasma levels. *B*: differences between concentrations of [^{3}H]dextran fractions in plasma and lymph specimens obtained during *hours 29.5–30.5* of same [^{3}H]dextran infusion as shown in *A*. Each point represents mean cpm/ml (bars indicate range and lack of bars indicates range < ± 50 cpm/ml) per fraction from single lymph and corresponding plasma sample both fractionated in duplicate. Within limits of variability of techniques there are no changes in absolute plasma or lymph concentrations for any fraction between 5.5- to 7.5-h period (*A*) and 29.5- to 30.5-h period.

the same sheep. Comparison of L/P ratios from the three collection periods shows that these L/P ratios remained essentially unchanged over time; in particular, no increase in L/P ratios occurred for the larger dextran fractions even when the infusion was continued to 30.5 h, i.e., to four times the duration of our standard collection period, indicating that the L/P ratios obtained during our standard period (5.5–7.5 h of infusion) were indistinguishable from steady-state values.

In Fig. 2 are given the radioactivities of the [^{3}H]-dextran fractions in plasma and lymph during *hours 5.5–7.5* and *29.5–30.5* for the animal whose L/P ratios are shown in Fig. 1. Again, the counts per minute per milliliter of plasma and lymph for all fractions were unchanging between the 5.5- to 7.5-h period and the 29.5- to 30.5-h period, confirming the steady-state nature of the corresponding L/P ratio. It is also evident in Fig. 2 that the low L/P ratios obtained for dextran fractions 5.2–8.4 nm in radius were primarily due to the very low levels of radioactivity in lymph rather than to inordinately high plasma levels.

As described in the example above we evaluated whether L/P ratios for the 5.5- to 7.5-h period of infusion changed over time by extending the duration of infusion

beyond our standard duration of 7.5 h. This was also done in three additional sheep. Table 3 lists the L/P ratios for all four sheep that received extended infusions and compares values for the 5.5- to 7.5-h period with those obtained from the last 1–1.5 h of each infusion. For all four sheep the L/P ratios did not change within the limits of our measurements, confirming that the values obtained from 5.5 to 7.5 h were steady-state values.

Finally, we evaluated whether the L/P ratios for the dextran fractions at *hours 5.5–7.5* of infusion differed significantly from values obtained from the preceding 2-h time period, i.e., *hours 3.5–5.5*. Figure 3 compares L/P ratios for *hours 5.5–7.5* with those for *hours 3.5–5.5* for the eight sheep in whom data were available for both time periods. The differences in L/P ratios for all 24 fractions from the two time periods were not statistically significant.

Based on the above lack of any substantial changes in L/P ratios for all dextran fractions between those obtained during *hours 5.5–7.5* compared with those obtained not only during the 2-h period immediately before but also after extending the infusions for up to 30 h, we have taken the L/P ratios obtained during *hours 5.5–7.5* to represent true steady-state values, i.e., values after full equilibration of the tracer has occurred between plasma and lymph, for purposes of further analysis and comparison.

TABLE 3. *L/P ratios for fractions of [^{3}H]dextrans in four sheep*

Molecular Radius, nm	*Sheep 21*		*Sheep 33*		*Sheep 97*		*Sheep 100*	
	5.5–7.5	11.5–13.0	5.5–7.5	13.5–15.0	5.5–7.5	29.5–30.5	5.5–7.5	27.5–29.0
1.6	1.14	0.99	1.08	0.94	1.07	0.94	1.09	1.09
1.8	1.11	0.98	1.00	0.89	1.09	0.96	1.06	0.97
2.0	1.05	1.01	0.85	0.78	1.05	0.91	0.78	0.85
2.2	0.93	0.87	0.72	0.66	1.00	0.88	0.48	0.71
2.4	0.80	0.69	0.58	0.53	0.92	0.70	0.35	0.56
2.6	0.62	0.57	0.45	0.41	0.78	0.59	0.26	0.42
2.8	0.44	0.48	0.35	0.31	0.60	0.52	0.20	0.31
3.0	0.34	0.37	0.26	0.23	0.46	0.40	0.15	0.22
3.2	0.23	0.27	0.19	0.17	0.36	0.28	0.13	0.16
3.4	0.15	0.19	0.13	0.12	0.28	0.21	0.13	0.12
3.6	0.10	0.14	0.086	0.088	0.21	0.15	0.11	0.10
3.8	0.065	0.10	0.061	0.070	0.15	0.11	0.10	0.088
4.0	0.042	0.075	0.041	0.050	0.10	0.078	0.10	0.081
4.2	0.036	0.054	0.030	0.032	0.075	0.058	0.098	0.076
4.4	0.028	0.040	0.024	0.028	0.054	0.043	0.097	0.073
4.8	0.011	0.020	0.016	0.021	0.031	0.026	0.098	0.069
5.2	0.008	0.018	0.014	0.018	0.019	0.018	0.097	0.067
5.6	0.009	0.014	0.013	0.016	0.013	0.011	0.091	0.066
6.0	0.009	0.013	0.013	0.016	0.010	0.008	0.085	0.062
6.4	0.006	0.007	0.009	0.018	0.008	0.007	0.078	0.055
6.8	0.006	0.007	0.007	0.022	0.007	0.007	0.069	0.051
7.2	0.010	0.013	0.011	0.024	0.006	0.007	0.061	0.049
7.8	0.016	0.024	0.024	0.033	0.006	0.009	0.057	0.045
8.4	0.024	0.030	*	*	0.006	0.009	0.061	0.046

Values compare lymph-to-plasma (L/P) ratios at *5.5–7.5 h* of infusion with those at more prolonged times, whose hours are listed. * Fraction inadvertently omitted from counting.

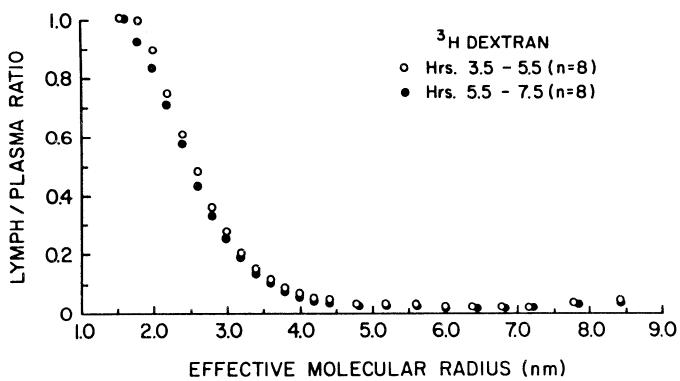

FIG. 3. Comparison of mean lymph-to-plasma (L/P) ratios (±SE) for uncharged [^{3}H]dextrans derived from lymph and plasma samples collected during *hours 3.5–5.5* (*open circles*) with those taken during *hours 5.5–7.5* (*closed circles*) of [^{3}H]dextran infusions in same 8 sheep. L/P ratios are not statistically different at any molecular radii ($P > 0.05$).

Molecular Sieving of [^{3}H]dextrans

The steady-state mean L/P ratios for [^{3}H]dextran fractions for all nine experimental animals are shown in Table 4. The results were consistent among all animals. The mean data shown in Fig. 4 are consistent with the findings described above for the representative infusion: *1*) the concentration of dextrans in the fractions ~1.6–1.8 nm in radius were approximately equal in lymph and plasma; *2*) molecular sieving occurred for dextran fractions >1.8 nm in radius; and *3*) L/P ratios for dextran fractions larger than 5.2 nm in radius were not distinguishable from zero. Also shown in Fig. 4 is the best-fit theoretical curve of L/P ratios predicted for uncharged solutes passing through a homoporous membrane. This curve was derived by assuming a simple one-pore model of an ideal semipermeable membrane through which uncharged solutes pass by convection and diffusion via cylindrical pores of a single theoretical pore radius and a single theoretical pore surface area per unit path length. The derivation of the model, calculations, and other results of this modeling are given and discussed in the APPENDIX. The theoretical curve fits the experimental data most closely at a theoretical pore radius of 5.0 nm and theoretical pore surface area-to-unit path length ratio of 2.6×10^4 cm.

Endogenous Proteins

In Fig. 5 the mean steady-state L/P ratios for [^{3}H]-dextrans for all nine infusions are compared with L/P ratios for endogenous albumin for five of the same nine sheep that received the dextran infusions and for seven endogenous protein fractions in eight awake sheep reported by Brigham et al. (4). In both laboratories the animal preparations were similar. A striking difference can be seen between the uncharged dextrans and the endogenous proteins in their L/P ratios for a given molecular radius. For example, the L/P ratio for albumin (effective molecular radius = 3.6 nm, Table 1) in our five sheep was 0.76 ± 0.01 compared with an L/P ratio of only 0.11 ± 0.02 for uncharged dextrans at the same radius; the difference in L/P ratios was highly statistically significant ($P < 10^{-6}$). The same result can be seen for the seven endogenous protein fractions reported by Brigham et al. (4). The L/P ratios for their protein fractions are much higher than those for uncharged dextran fractions at the same or next larger molecular

TABLE 4. *Steady-state L/P ratios for fractions of [^{3}H]dextrans in nine sheep*

Molecular Radius, nm	Lymph Flow, ml/h										
	5.7	4.4	12.5	4.9	4.8	9.6	3.7	16.2	4.4	7.4±1.5	
	Sheep 9 (30.0 kg)	*Sheep 13* (29.2 kg)	*Sheep 21* (44.5 kg)	*Sheep 25* (36.0 kg)	*Sheep 33* (42.6 kg)	*Sheep 42* (41.0 kg)	*Sheep 56* (22.0 kg)	*Sheep 97* (52.0 kg)	*Sheep 100* (33.0 kg)	Mean±SE (36.7±3.1 kg)	
1.6	1.13	1.06	1.14	0.85	1.08	0.80	0.93	1.07	1.09	1.02	0.04
1.8	1.05	1.03	1.11	0.88	1.00	0.79	0.91	1.09	1.06	0.99	0.04
2.0	0.93	0.91	1.05	0.86	0.85	0.67	0.93	1.05	0.78	0.89	0.04
2.2	0.75	0.79	0.93	0.75	0.72	0.55	0.85	1.00	0.48	0.76	0.06
2.4	0.52	0.60	0.80	0.61	0.58	0.46	0.74	0.92	0.35	0.62	0.06
2.6	0.36	0.41	0.62	0.48	0.45	0.38	0.54	0.78	0.26	0.48	0.05
2.8	0.25	0.28	0.44	0.35	0.35	0.31	0.48	0.60	0.20	0.36	0.04
3.0	0.18	0.18	0.34	0.26	0.26	0.24	0.43	0.46	0.15	0.28	0.04
3.2	0.12	0.12	0.23	0.18	0.19	0.17	0.34	0.36	0.13	0.20	0.03
3.4	0.08	0.070	0.15	0.12	0.13	0.13	0.27	0.28	0.13	0.15	0.03
3.6	0.060	0.050	0.10	0.075	0.086	0.096	0.20	0.21	0.11	0.11	0.02
3.8	0.052	0.038	0.065	0.062	0.061	0.066	0.15	0.15	0.10	0.083	0.014
4.0	0.059	0.028	0.042	0.040	0.041	0.044	0.12	0.10	0.10	0.062	0.011
4.2	0.043	0.028	0.036	0.025	0.030	0.033	0.10	0.075	0.098	0.051	0.010
4.4	0.038	0.020	0.028	0.013	0.024	0.030	0.072	0.054	0.097	0.041	0.009
4.8	0.036	0.015	0.011	0.007	0.016	0.020	0.064	0.031	0.097	0.032	0.010
5.2	0.045	0.022	0.008	0.005	0.014	0.018	0.061	0.014	0.097	0.031	0.010
5.6	0.044	0.022	0.009	0.005	0.013	0.012	0.049	0.013	0.091	0.028	0.009
6.0	0.042	0.015	0.009	0.002	0.013	0.018	0.042	0.010	0.085	0.026	0.009
6.4	0.047	0.011	0.006	0.002	0.009	0.022	0.040	0.008	0.078	0.025	0.008
6.8	0.049	0.015	0.006	0.001	0.007	0.020	0.039	0.007	0.069	0.024	0.008
7.2	0.056	0.024	0.010	0.001	0.011	0.028	0.038	0.006	0.061	0.026	0.007
7.8	0.072	0.042	0.016	0.010	0.024	0.052	0.028	0.006	0.057	0.034	0.008
8.4	0.088	0.060	0.024	0.030	*	0.092	0.025	0.006	0.061	0.048	0.011

Values of lymph-to-plasma (L/P) ratios are derived from samples collected over *hours 5.5–7.5* of [^{3}H]dextran infusion. * Fraction omitted inadvertently from counting.

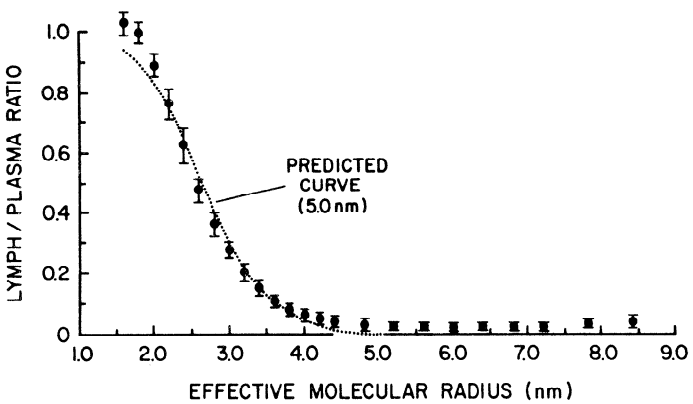

FIG. 4. Mean steady-state lymph-to-plasma (L/P) ratios (±SE) of uncharged [^{3}H]dextran fractions according to effective molecular radii during *hours 5.5–7.5* of infusions in 9 sheep. Results are consistent with molecular sieving of tracer from plasma to lymph. *Dotted line* represents theoretical curve for molecular sieving of dextrans through ideal homoporous membrane with cylindrical pores of 5.0-nm radius. Theoretical curve was derived by "best-fit" estimate comparing theoretical lymph-to-plasma (L/P) ratios with experimental L/P ratios for [^{3}H]dextran fractions shown (see text and APPENDIX for details of mathematical model).

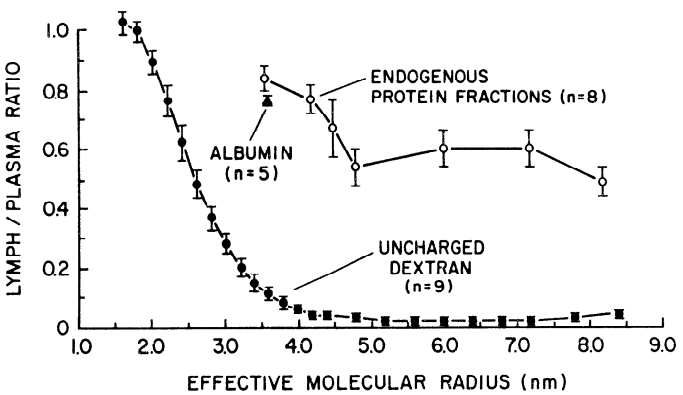

FIG. 5. Comparison of mean steady-state L/P ratios (±SE) for fractions of [^{3}H]dextrans in 9 sheep to mean lymph-to-plasma (L/P) ratio (±SE) for endogenous albumin measured in 5 of same 9 sheep and for 7 endogenous protein fractions in 8 similarly prepared sheep by Brigham et al. (4). L/P ratios for albumin and for all endogenous protein fractions are much higher from those for [^{3}H]dextrans at same or next larger effective molecular radius. Differences are statistically significant ($P < 10^{-5}$). Lines have been added for clarity.

radius; all these differences were also highly statistically significant ($P < 10^{-5}$).

DISCUSSION

The present study in awake intact sheep examined the effect of variations in molecular size of uncharged macromolecules ([^{3}H]dextrans) on their movement between pulmonary microcirculation, i.e., the minute vessels of the lungs engaged in the exchange of water and macromolecules between lumen and interstitium and the efferent lymphatic of the caudal mediastinal lymph node. In addition to their lack of charge the use of dextrans had two other attractive features: *1*) their availability as a polydisperse mixture of different molecular sizes made it possible to investigate a range of effective molecular radii during a single experiment; and *2*) their previous use by others as tracers in organs other than the lungs (18, 27) made it possible for us to compare our results on the

lungs with those made on the liver, intestine, and hindlimb.

Uncertainties About the Sheep Preparation

One uncertainty inherent in the animal preparation that we used is the prospect that pulmonary lymph may be contaminated by systemic lymph (34). We attempted to minimize this possibility by surgically interrupting the right and left transdiaphragmatic lymphatics that anastomose with the caudal mediastinal lymph node. That we succeeded in minimizing lymph contamination from intra-abdominal sources in our preparations was supported by the virtual absence of dextran fractions >5.0 nm in radius in the lymph that we collected compared with the high L/P ratios in liver lymph and intestinal lymph reported by others (27) (Fig. 6).

A second uncertainty stems from the fact that the pulmonary lymph that we collected is postnodal, raising the possibility that passage through the node may have changed lymph volume or composition. That appreciable change in the concentration of lymph does not occur because of passage through the caudal mediastinal node is indicated by the recent demonstration that the concentration of ^{125}I-bovine albumin in the afferent and efferent lymphatics of this preparation are virtually identical (36). Also against an important role for dilution of lymph in our experiments are two considerations: *1*) even if dilution of lymph did occur the L/P ratios of the dextrans and endogenous proteins would be expected to be diluted to the same degree; and *2*) our observations that the concentration of [^{3}H]dextrans is virtually zero in fractions >5.0 nm in radius, an observation not accountable by simple dilution of lymph alone. The opposite possibility, that dextrans are taken up by the caudal mediastinal lymph node, is more difficult to discount because direct experiments on the caudal mediastinal node have not been done. However, the popliteal node of the dog does not take up dextrans of the size that we used or larger (26).

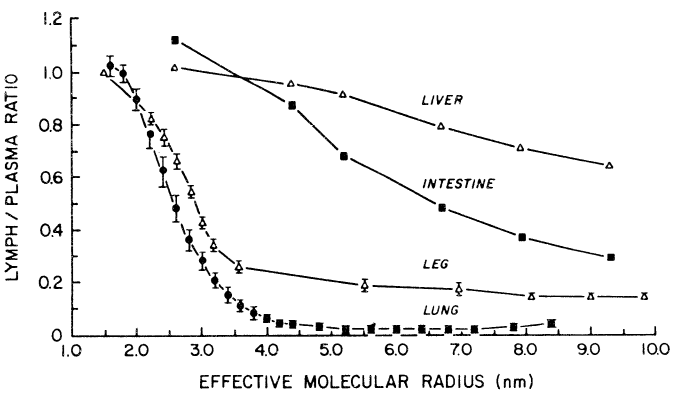

FIG. 6. Comparison of mean lymph-to-plasma (L/P) ratios (±SE if available) for uncharged dextrans according to effective molecular size in different organs. For all organs except lung, L/P ratios for fractions of dextrans >5.0 nm in radius are substantially above 0, suggesting large pore pathway for dextrans in these organs (18, 27). L/P ratios for lung are from present study (n = 9), data for leg are from Grotte (n = 13) (18), and data for intestine (n = 26) and liver (n = 23) are from Mayerson et al. (27). Effective molecular radii used for dextran fractions for organs other than lung were either those given in original study (18) or those calculated on basis of authors' published molecular weights (27) by use of linear regression equation relating log (dextran molecular weight) vs. log (dextran effective molecular radius), employing data of Granath (16) and of Laurent and Granath (23). Lines have been added for clarity.

Comparison of L/P Ratios of Uncharged Dextrans and of Endogenous Proteins

As noted above (Fig. 5) the steady-state transport of plasma proteins between the pulmonary circulation and lung lymph is greater than that of uncharged dextrans of the same effective molecular size. For this comparison we pooled our observations using albumin with those of Brigham, Bowers, and Haynes (4), who used plasma proteins. The following criteria need to be met to validate the comparison: the experimental preparations and circumstances must have been comparable with respect to the type of animal preparations, Starling forces (hydrostatic and oncotic pressures), and methods for determining effective molecular size; and the L/P ratios for uncharged dextrans like endogenous proteins were obtained under steady-state conditions.

That the animal preparations were comparable is indicated on two accounts: *1*) except for the fourth thoracotomy to minimize contamination of pulmonary lymph by systemic lymph, the surgical manipulations were the same in both preparations; and *2*) our L/P ratios for albumin and total protein (Table 2) did not differ statistically from those reported by Brigham et al. (4). The criterion of comparable Starling forces also seems to have been satisfied, since mean pulmonary arterial, left atrial pressures, rates of lymph flow, and L/P ratios for albumin and total protein were quite similar. The criterion for comparable effective molecular radii also seems to have been satisfied, since values for effective molecular sizes were checked directly in both studies against similar protein standards.

The final criterion for comparing dextran and protein data was that the L/P ratios for uncharged dextrans were steady-state values. That our experiments satisfied this condition is indicated by the lack of changes in mean L/P ratios (at any radius) between values obtained at 5.5–7.5 h (standard collection period) and those obtained later (up to 30.5 h) (Figs. 1 and 2 and Table 3). Longer equilibration times appear to be required for labeled proteins (10) than for dextrans possibly due to ionic interactions with cell membranes and interstitium (35).

Explanation of Different L/P Ratios for Dextrans and Proteins

With respect to the questions posed in this study at least three physicochemical differences distinguish plasma proteins from dextrans: *1*) electrical charge, since all but a few plasma proteins are amphoteric molecules that are negatively charged at physiological pH (33); *2*) greater flexibility of dextran molecules than of protein molecules; and *3*) molecular shape, since dextrans in solution move as relatively spherical masses composed of a randomly coiled polysaccharide chain and enveloped water molecules (16), whereas some plasma proteins with

the same effective molecular radius are ellipsoid in shape and may move parallel to their major axes (33). Of these three only the net electrical charge or amphoteric nature of proteins seems likely to explain the enhanced transcapillary passage of endogenous plasma proteins compared with [^{3}H]dextran between the lungs and efferent lymph of the caudal mediastinal lymph node. Support for this conclusion has been provided by recent reports of greater pulmonary plasma-to-lymph passage of anionic dextrans (15, 22) than of uncharged dextrans.

Applicability of Pore Concept to Present Study

As indicated above (Fig. 4) our study showed that the passage of uncharged dextrans above 5.0 nm in molecular radius appears to be markedly restricted. This observation suggests that the large pores (18, 27) that account for the passage of the proteins [and dextrans in other organs (Fig. 6)] are unavailable for appreciable transendothelial passage of the uncharged dextrans in the lung.

Our results along this line differ from those obtained in two other laboratories that also used exogenous nonprotein tracers in the pulmonary microcirculation (3, 28). In the study of Boyd et al. (3) an uncharged polydisperse macromolecular tracer, ^{125}I-polyvinylpyrrolidone (^{125}I-PVP), was injected as a single bolus and the data were not collected in a steady state. Although the latter makes direct comparisons of L/P ratios of fractions of ^{125}I-PVP with our results more difficult, it is evident that much larger percentages of plasma concentrations of ^{125}I-PVP (>4.0 nm in radius) were found in the lymph than we found for [^{3}H]dextrans. Two reasons may explain the differences: *1*) the ^{125}I-PVP studies utilized an anesthetized fetal lamb preparation raising the possibility that the lungs are more permeable to the larger macromolecules due to prior tracheal clamping and acute surgical manipulation; and *2*) the collection of lymph in the fetal lambs did not exclude the possibility of contamination of pulmonary lymph (34) by intra-abdominal systemic lymph, which has higher L/P ratios for the large dextran fractions (Fig. 6) (18, 27), since both the left and right transdiaphragmatic anastomoses with the caudal mediastinal lymph node were left intact.

The other discrepant study (28) also differed importantly with respect to experimental method and preparation: use of a larger injectate, i.e., 2.0–2.5 g of dextrans of larger molecular weight; labeling of the tracer with fluorescein isothiocyanate (FITC) and subsequent intravenous administration as a bolus; and use of an acute anesthetized sheep preparation 1.5 days later to collect efferent caudal mediastinal lymph. Three reasons could account for the different results. First, nodal anastamoses of the hepatic lymphatics (by way of left transdiaphragmatic lymphatics) with high L/P ratios for dextran fractions of 10.0 nm in radius (27) were not surgically interrupted, since such contaminating systemic lymphatics have been found to contribute up to 30% of the total efferent lymph flow in the anesthetized sheep preparation (34). Second, surgical manipulation of the right lung immediately prior to lymph collection entails a risk of increasing capillary permeability. Finally, dextrans labeled with FITC become charged because the fluorescein moiety is anionic at physiological pH due to dissociation of its carboxylic acid group (8); as a result, blood-to-lymph transport may be enhanced (15, 22).

In contrast to the two studies described above, our results, which indicate a size-selective pathway in the pulmonary microcirculation with an equivalent pore radius of about 5.0 nm for uncharged molecules, do agree with those of Taylor and Gaar (41). Although they used an entirely different experimental approach, i.e., measuring of osmotic reflection coefficients for urea, glucose, and sucrose, on the basis of results from use of these uncharged nonprotein solutes, they calculated an equivalent pore radius between 4.0 and 5.8 nm for the pulmonary microcirculation (41).

The Sites of the Selective Pathways for Size and Charge

The components of the pulmonary microcirculation involved in the passage of fluid and macromolecules from plasma to pulmonary lymph are generally considered to be predominantly the pulmonary capillaries. Moreover, at least two separate pathways have been proposed to account for the transport of macromolecules across the pulmonary capillary endothelium: intercellular junctions and the system of plasmalemmal vesicles. However, at present the relative contributions made by these two categories of pathways to either protein transport or dextran transport across the pulmonary endothelium are unclear. Our studies leave unsettled the pathways for either proteins or dextrans, the loci on the cell surface that are involved, and their mechanisms of transport. Moreover, it is likely that the depiction of macromolecular transport from blood to lung lymph will need to incorporate not only pathways through pulmonary endothelium but also pathways through the capillary endothelial basement membrane, the extracellular matrix of the interstitial space, and afferent lymphatics, since these are also part of the blood-to-lymph barrier. Electrical charges not only on the endothelial luminal surface (32) but also on the endothelial basement membrane (45) and in the interstitial extracellular matrix (44) can be expected to influence importantly the movement of charged vs. uncharged macromolecules from plasma to afferent lymphatics.

APPENDIX

Derivation and application of an equivalent pore membrane model

The model is based on the following assumptions: *1*) that steady-state transport of water and an uncharged solute across a biological membrane is described by the Kedem-Katchalsky coupled solvent-solute equations (20) [these equations were subsequently rewritten by Patlak et al. (31) in differential form and integrated across the membrane thickness]; *2*) that total net transmembrane solvent flow is equal to lymph flow; and *3*) that transmembrane solute flow is equal to the product of lymph flow times solute concentration in lymph.

The above three assumptions result in the following theoretical relationship of the form reported by Granger and Taylor (17)

$$\frac{C_L}{C_P} = \frac{1 - \sigma_f}{(1 - \sigma_f)e^{-x}}, \qquad \text{with } x = \frac{(1 - \sigma_f)J_L}{PS} \tag{1}$$

where C_L and C_P are the concentrations of a single solute in lymph and

plasma, respectively, at full equilibrium, σ_f is the solute's solvent drag reflection coefficient, J_L is the lymph flow, and PS is the solute's permeability-surface area product.

A single-pore model of membrane structure was used to describe the sieving characteristics of the L/P ratios for the dextran fraction data. This model assumed that dextran molecules can be described as rigid spheres passing through a semipermeable membrane via cylindrical water-filled pores of a single unknown radius, length, and number. The transport properties of this equivalent membrane structure were included by use of the following expressions for σ_f and PS (2, 19, 29)

$$\sigma_f = 1 - [2(1 - \alpha)^2 - (1 - \alpha)^4]\kappa_2/\kappa_1 \quad (2)$$

$$PS = (1 - \alpha)^2 \cdot \frac{A}{\Delta x} \cdot \frac{D_f}{\kappa_1} \quad (3)$$

where α is the ratio of the solute's equivalent hydrodynamic (Stokes-Einstein) radius (a_s) to the theoretical pore radius (r), $A/\Delta x$ is the radio of the surface area of the pores to the length of the pore, D_f is the solute's free diffusion coefficient, and κ_1 and κ_2 are the tabulated values as a function of α reported by Paine and Scherr (29). These were derived in the course of their numerical solution to transport of rigid spheres through pores with this geometry. Thus in *Eqs. 2* and *3*, σ_f and PS are functions only of solute size and pore size, number, and length.

A particular assumption for this model is that, for a given solute size and pore size, σ_f is a constant and equal to σ_d, the solute's osmotic reflection coefficient. This assumption is justifiable because our model is a homoporous, rather than heteroporous, membrane (42).

The above expressions for σ_f and PS and the Stokes-Einstein equation for D_f were substituted in *Eq. 1* to give the following theoretical relationship for a given solute

$$\frac{C_L}{C_P} = \frac{[2(1 - \alpha)^2 - (1 - \alpha)^4]\kappa_2/\kappa_1}{1 - \{1 - [2(1 - \alpha)^2 - (1 - \alpha)^4]\kappa_2/\kappa_1\} \cdot \exp\{[(1 - \alpha)^2 - 2]\kappa_2 \cdot a_2 \cdot \gamma\}} \quad (4)$$

where $\gamma = J_L \cdot 6\pi\eta/kT \cdot \Delta x/A$ (η is solvent viscosity, k is the Boltzmann constant, and T is absolute temperature, °K).

The two free parameters in *Eq. 4* are the theoretical pore radius r and γ. The sum of squares of the difference between the theoretically predicted values (*Eq. 4*) and the experimental data (Table 4) was minimized when $r = 5.0$ nm and $\gamma = 2.3 \times 10^5$ cm^{-1}.

These parameter values were then used to estimate $A/\Delta x$ by solving for $A/\Delta x$ in the above expression for γ. With γ of 2.3×10^5 cm^{-1}, J_L (mean lymph flow during 9 infusions) of 2.06×10^{-3} cm$^3 \cdot$s^{-1} (Table 2), T (mean temperature of sheep) of 312.7°K, η (viscosity of water at 312.7°K) of 6.7×10^{-3} g$\cdot$cm$^{-1}\cdot$s^{-1}, k of 1.38×10^{-16} g$\cdot$cm$^2\cdot$s$^{-2}\cdot$°K^{-1}, $A/\Delta x$ was found to equal 2.6×10^4 cm.

By use of quantitative morphological measurements these results can be further interpreted to estimate the numerical relationship between number of pores and number of pulmonary capillary endothelial cells. If $\Delta x = 0.5$ μm, which is the average thickness of endothelium in most mammalian species (47), then the total pore surface area, A, is 1.3 cm^2 and the total number, N, of equivalent pores is 1.6×10^{12}. The pulmonary capillary surface area containing these pores can be estimated at roughly 50 m^2 by substituting the total pulmonary capillary surface of the goat, ~100 m^2 (47), for that of the sheep, since ovine data are unavailable, and by using values of Erdmann et al. (13) that 50% of the total lung on the average is drained by the caudal mediastinal lymph node. Thus the total pore surface area, 1.3 cm^2, represents a very small fraction of the corresponding pulmonary capillary surface area, only about 0.0003 of 1%. Finally, by dividing this 50-m^2 surface area by the mean surface area for a single pulmonary capillary endothelial cell, 1,000 μm^2 (14), we estimate that, on the average, each endothelial cell is associated with ~32 equivalent pores.

We gratefully acknowledge the advice of Eugene M. Renkin, the assistance of Michael G. Magno and Dennis A. Silage, the data processing and technical skills of Thomas Langan, the technical contributions of Mary O'Brien, Daniel Gonder, and Mercedes Lee, and the secretarial skill of Daniel Barrett.

This work was supported by National Heart, Lung, and Blood Institutes Grant HL-08805 and a Special Investigatorship from the American Heart Association.

Received 23 February 1984; accepted in final form 4 March 1985.

REFERENCES

1. ATLAS, S. M., AND E. FARBER. On the molecular weight of cytochrome *c* from mammalian heart muscle. *J. Biol. Chem.* 219: 31–37, 1956.
2. BEAN, C. P. Physics of porous membranes. In: *Membranes: a Series of Advances*, edited by C. Eisenman. New York: Dekker, 1972, vol. 7, p. 1–54.
3. BOYD, R. H. D., J. R. HILL, P. W. HUMPHREYS, I. C. S. NORMAND, E. O. R. REYNOLDS, AND L. B. STRANG. Permeability of lung capillaries to macromolecules in foetal and new-born lambs and sheep. *J. Physiol. London* 201: 567–588, 1969.
4. BRIGHAM, K. L., R. E. BOWERS, AND J. HAYNES. Increased sheep lung vascular permeability caused by *Escherichia coli* endotoxin. *Circ. Res.* 45: 292–297, 1979.
5. CHANG, R. L. S., W. M. DEEN, C. R. ROBERTSON, AND B. M. BRENNER. Permeability of the glomerular capillary wall. III. Restricted transport of polyanions. *Kidney Int.* 8: 212–218, 1975.
6. CHANG, R. L. S., I. F. UEKI, J. L. TROY, W. M. DEEN, C. R. ROBERTSON, AND B. M. BRENNER. Permselectivity of the glomerular capillary wall to macromolecules. II. Experimental studies in rats using neutral dextrans. *Biophys. J.* 15: 887–906, 1975.
7. CREETH, J. M. Studies of free diffusion in liquids with the Rayleigh method. III. The analysis of known mixtures and some preliminary investigations with proteins. *J. Phys. Chem.* 62: 66–74, 1958.
8. DEBELDER, A. N., AND K. GRANATH. Preparation and properties of fluorescein-labelled dextrans. *Carbohydrate Res.* 30: 375–378, 1973.
9. DE LA HUERGA, J., G. W. SMETTERS, AND J. C. SHERRICK. Colorimetric determination of serum proteins: the buiret reaction. In: *Serum Proteins and the Dysproteinemias*, edited by F. W. Sunderman and F. W. Sunderman, Jr. Philadelphia, PA: Lippincott, 1964, p. 52–62.
10. DEMLING, R. H., S. L. SELINGER, R. D. BLAND, AND N. C. STAUB. Effect of acute hemorrhagic shock on pulmonary microvascular fluid filtration and protein permeability in sheep. *Surgery* 77: 512–519, 1975.
11. DREYWOOD, R. Qualitative test for carbohydrate material. *Ind. Eng. Chem. Anal. Ed.* 18: 499, 1946.
12. EDELHOCH, H. The properties of thyroglobulin. I. The effects of alkali. *J. Biol. Chem.* 235: 1326–1340, 1960.
13. ERDMANN, A. J., III, T. R. VAUGHAN, JR., K. L. BRIGHAM, W. C. WOOLVERTON, AND N. C. STAUB. Effect of increased vascular pressure on lung fluid balance in unanesthetized sheep. *Circ. Res.* 37: 271–284, 1975.
14. GIL, J., D. A. SILAGE, AND J. M. MCNIFF. Distribution of vesicles in cells of air-blood barrier in the rabbit. *J. Appl. Physiol.* 50: 334–340, 1981.
15. GLAUSER, F. L., R. P. FAIRMAN, AND J. E. MILLEN. Facilitated transport of anionic dextrans in the pulmonary microvasculature of sheep. *Microcirculation* 2: 305–313, 1982.
16. GRANATH, K. A. Solution properties of branched dextrans. *J. Colloid Sci.* 13: 308–328, 1958.
17. GRANGER, D. N., AND A. E. TAYLOR. Permeability of intestinal capillaries to endogenous macromolecules. *Am. J. Physiol.* 238 (*Heart Circ. Physiol.* 7): H457–H464, 1980.
18. GROTTE, G. Passage of dextran molecules across the blood-lymph barrier. *Acta Chir. Scand. Suppl.* 211: 1–84, 1956.
19. HARRIS, T. R., AND R. J. ROSELLI. A theoretical model of protein, fluid, and small molecule transport in the lung. *J. Appl. Physiol.* 50: 1–14, 1981.
20. KEDEM, O., AND A. KATCHALSKY. Thermodynamic analysis of the permeability of biological membranes to non-electrolytes. *Biochim. Biophys. Acta* 27: 229–246, 1958.
21. LAMM, O., AND A. POLSON. The determination of diffusion constants of proteins by a refractometric method. *Biochem. J.* 30: 528–541, 1936.
22. LANKEN, P. N., P. M. SAMPSON, J. H. HANSEN-FLASCHEN, M. MAGNO, A. P. FISHMAN, AND G. G. PIETRA. Effect of charge on movement of macromolecules from plasma to lung lymph: facili-

tation of dextran sulfate (Abstract). *Federation Proc.* 41: 1247, 1982.
23. LAURENT, T. C., AND K. A. GRANATH. Fractionation of dextran and ficoll by chromatography on Sephadex G-200. *Biochim. Biophys. Acta* 136: 191–198, 1967.
24. LAURENT, T. C., AND J. KILLANDER. A theory of gel filtration and its experimental verification. *J. Chromatogr.* 14: 317–330, 1964.
25. MANCINI, G., A. O. CARBONARA, AND J. F. HEREMANS. Immunochemical quantitation of antigens by single radial immunodiffusion. *Immunochemistry* 2: 235–254, 1965.
26. MAYERSON, H. S., R. M. PATTERSON, A. MCKEE, S. J. LEBRIE, AND P. MAYERSON. Permeability of lymphatic vessels. *Am. J. Physiol.* 203: 98–106, 1962.
27. MAYERSON, H. S., C. G. WOLFRAM, H. H. SHIRLEY, JR., AND K. WASSERMAN. Regional differences in capillary permeability. *Am. J. Physiol.* 198: 155–160, 1960.
28. MCNAMEE, J. E. Restricted dextran transport in the sheep lung lymph preparation. *J. Appl. Physiol.* 52: 585–590, 1982.
29. PAINE, P. L., AND P. SCHERR. Drag coefficients for the movement of rigid spheres through liquid-filled cylindrical pores. *Biophys. J.* 15: 1087–1091, 1975.
30. PARKER, J. C., R. E. PARKER, D. N. GRANGER, AND A. E. TAYLOR. Vascular permeability and transvascular fluid and protein transport in the dog lung. *Circ. Res.* 48: 549–561, 1981.
31. PATLAK, C. S., D. A. GOLDSTEIN, AND J. F. HOFFMAN. The flow of solute and solvent across a two-membrane system. *J. Theor. Biol.* 5: 426–442, 1963.
32. PIETRA, G. G., P. SAMPSON, P. N. LANKEN, J. HANSEN-FLASCHEN, AND A. P. FISHMAN. Transcapillary movement of cationized ferritin in the isolated perfused rat lung. *Lab. Invest.* 49: 54–61, 1983.
33. PUTNAM, F. W. Alpha, beta, gamma, omega—the roster of the plasma proteins. In: *The Plasma Proteins. Structure, Function and Genetic Control*, edited by F. W. Putnam. New York: Academic, 1975, vol. 1, p. 57–131, 1975.
34. ROOS, P. J., J. P. WIENER-KRONISH, K. H. ALBERTINE, AND N. C. STAUB. Removal of abdominal sources of caudal mediastinal node lymph in anesthetized sheep. *J. Appl. Physiol.* 55: 996–1001, 1983.
35. SCHNEEBERGER, E. E. Circulating proteins and macromolecular transport across continuous nonfenestrated endothelium. *Ann. NY Acad. Sci.* 40: 25–37, 1982.
36. SCHULTZ, E. L., K. H. ALBERTINE, AND N. C. STAUB. Protein concentration in afferent and efferent lymph of caudal mediastinal node in sheep (Abstract) *Microvasc. Res.* 3: 256, 1983.
37. SCHWERT, G. W. The molecular size and shape of the pancreatic proteases. *J. Biol. Chem.* 190: 799–806, 1951.
38. STAUB, N. C., R. D. BLAND, K. L. BRIGHAM, R. DEMLING, A. J. ERDMANN III, AND W. C. WOOLVERTON. Preparation of chronic lung lymph fistulas in sheep. *J. Surg. Res.* 19: 315–320, 1975.
39. STERN, K. G., S. SINGER, AND S. DAVIS. A diffusion cell adapted to use in the Tiselius apparatus. *J. Biol. Chem.* 167: 231–330, 1947.
40. SUMNER, J. B., AND N. GRALEN. The molecular weight of crystalline catalase. *J. Biol. Chem.* 125: 33–36, 1938.
41. TAYLOR, A. E., AND K. A. GAAR, JR. Estimation of equivalent pore radii of pulmonary capillary and alveolar membranes. *Am. J. Physiol.* 218: 1133–1140, 1970.
42. TAYLOR, A. E., D. N. GRANGER, AND R. A. BRACE. Analysis of lymphatic protein flux data. I. Estimation of the reflection coefficient and permeability surface area product for total protein. *Microvasc. Res.* 13: 297–313, 1977.
43. TAYLOR, J. F., AND C. LOWRY. The molecular weights of some crystalline enzymes from muscle and yeast. I. Aldolase and D-glyceraldehyde-3-phosphate dehydrogenase. *Biochim. Biophys. Acta* 20: 109–117, 1956.
44. VACCARO, C. A., AND J. S. BRODY. Ultrastructural localization and characterization of proteoglycans in the pulmonary alveolus. *Am. Rev. Respir. Dis.* 120: 901–910, 1979.
45. VACCARO, C. A., AND J. S. BRODY. Structural features of alveolar wall basement membrane in the adult rat lung. *J. Cell Biol.* 91: 427–437, 1981.
46. VALLEE, B. L., AND W. E. C. WACKER. Metalloproteins. In: *The Proteins. Compositon, Structure and Function*, edited by H. Neurath. New York: Academic, 1967, vol. 5, p. 40.
47. WEIBEL, E. R. Morphological basis of alveolar-capillary gas exchange. *Physiol. Rev.* 53: 419–495, 1973.